Molecular Psychiatry (2015), 1–12

www.nature.com/mp

ORIGINAL ARTICLE

Dysregulation of miR-34a links neuronal development to genetic risk factors for bipolar disorder

S Bavamian[1,2,7], N Mellios[3,7], J Lalonde[1,2,4,7], DM Fass[1,2], J Wang[1,2,5,6], SD Sheridan[1,2,4,5,6], JM Madison[1,2,5], Fen Zhou[1,2,5], EH Rueckert[1,2,5], D Barker[2], RH Perlis[1,2,5,6], M Sur[3] and SJ Haggarty[1,2,4,5,6]

Bipolar disorder (BD) is a heritable neuropsychiatric disorder with largely unknown pathogenesis. Given their prominent role in brain function and disease, we hypothesized that microRNAs (miRNAs) might be of importance for BD. Here we show that levels of miR-34a, which is predicted to target multiple genes implicated as genetic risk factors for BD, are increased in postmortem cerebellar tissue from BD patients, as well as in BD patient-derived neuronal cultures generated by reprogramming of human fibroblasts into induced neurons or into induced pluripotent stem cells (iPSCs) subsequently differentiated into neurons. Of the predicted miR-34a targets, we validated the BD risk genes ankyrin-3 (*ANK3*) and voltage-dependent L-type calcium channel subunit beta-3 (*CACNB3*) as direct miR-34a targets. Using human iPSC-derived neuronal progenitor cells, we further show that enhancement of miR-34a expression impairs neuronal differentiation, expression of synaptic proteins and neuronal morphology, whereas reducing endogenous miR-34a expression enhances dendritic elaboration. Taken together, we propose that miR-34a serves as a critical link between multiple etiological factors for BD and its pathogenesis through the regulation of a molecular network essential for neuronal development and synaptogenesis.

Molecular Psychiatry advance online publication, 27 January 2015; doi:10.1038/mp.2014.176

INTRODUCTION

Bipolar disorder (BD) is a genetically complex neuropsychiatric disorder affecting approximately 2–4% of the population that is characterized by recurrent episodes of depression and mania or hypomania.[1,2] Although common- and rare-variant genetic association studies have begun to identify genes with variants conferring risk for developing BD, the pathogenesis of BD at a cellular level remains elusive. As a consequence, therapeutic options for BD are limited, consisting mainly of mood stabilizers developed decades ago, which are only effective in a subset of patients.

Recently, microRNAs (miRNAs), which are small, endogenous, non-coding RNAs of 18–23 nucleotides that posttranscriptionally regulate gene expression and are highly expressed in the brain,[3–7] have emerged as essential regulators of neuronal development, differentiation and neuroplasticity.[6,8–11] Understanding the function of miRNAs has led to the recognition of their ability to fine-tune the expression of numerous genes and orchestrate the overall activity of multiple pathway components, thereby positioning them to link numerous genetic risk factors for complex human genetic disorders into functional networks. An abundant literature now links miRNAs to neuropsychiatric disorders, especially through the analysis of the 22q11.2 schizophrenia susceptibility locus encompassing the miRNA processing gene *DGCR8*.[12–15] Moreover, alterations in miRNA profile have been identified in several psychiatric diagnoses, including schizophrenia, autism, depression, addiction and anxiety.[6,8,10,11,16–18] Indeed, recent evidence has shown that miR-137, a miRNA located within a locus that is associated with schizophrenia, may target a subset of important disease-related genes[19,20] and potentially explain phenotypic heterogeneity.[21,22] However, it remains unclear whether the single-nucleotide polymorphisms in this region implicate miR-137 itself or an adjacent gene.[23]

In the context of BD pharmacology, miR-34a, which belongs to the broadly evolutionarily conserved miR-34 microRNA family, has been shown to be reduced by lithium and valproic acid, two chemically distinct medications commonly used in the long-term treatment of BD.[24,25] Moreover, miR-34a can influence mouse neuronal development,[26] and its validated targets have been shown to be involved in neuronal differentiation, synaptic plasticity and long-term memory in mammals.[27–29] On the basis of these findings, we hypothesized that miR-34a could serve as an important link between emerging genetic risk factors for BD. Here we show that miR-34a levels are increased in the cerebellum of BD subjects as well as in human neuronal cultures from reprogrammed patient cells. In addition, we provide evidence that miR-34a targets BD-related genes *ANK3* and *CACNB3* and regulates their expression during neuronal differentiation. Elevation of miR-34a expression in human induced pluripotent stem cell (iPSC)-derived neuronal progenitors affected *ANK3* and *CACNB3* mRNA and protein expression and resulted in defects in neuronal differentiation as measured morphologically and biochemically through analysis of presynaptic and postsynaptic markers. Conversely, suppression of miR-34a expression enhanced

[1]Chemical Neurobiology Laboratory, Center for Human Genetics Research, Massachusetts General Hospital, Boston, MA, USA; [2]Stanley Center for Psychiatric Research, Broad Institute of MIT and Harvard, Cambridge, MA, USA; [3]Department of Brain and Cognitive Sciences, Picower Institute for Learning and Memory, Massachusetts Institute of Technology, Cambridge, MA, USA; [4]Department of Neurology, Massachusetts General Hospital, Harvard Medical School, Boston, MA, USA; [5]Department of Psychiatry, Massachusetts General Hospital, Harvard Medical School, Boston, MA, USA and [6]Center for Experimental Drugs and Diagnostics, Massachusetts General Hospital, Harvard Medical School, Boston, MA, USA. Correspondence: Professor SJ Haggarty, Chemical Neurobiology Laboratory, Center for Human Genetics Research, Massachusetts General Hospital, 185 Cambridge Street, Boston, MA 02114, USA.
E-mail: shaggarty@mgh.harvard.edu
[7]These authors contributed equally to this work.
Received 14 November 2013; revised 30 September 2014; accepted 12 November 2014

dendritogenesis. Expanded profiling of the consequence of miR-34a overexpression revealed effects on a number of additional genes critical to neurodevelopment and implicated in the etiology of BD by recent human genetic studies.[16,30] Taken together, our data highlight miR-34a as an important miRNA for BD and expand the knowledge on its effects on neuronal development.

MATERIALS AND METHODS

Postmortem human brain sample collection and RNA extraction

RNA samples (1–2 μg) from the frontal cortex (BA9; 33 control and 31 BD samples), anterior cingulate cortex (29 control and 29 BD samples) and cerebellum (lateral cerebellar hemisphere; 34 control and 29 BD samples) were obtained from the Stanley Medical Research Institute (Chevy Chase, MD, USA) Array Collection. Quality and concentration of total RNA was measured using a NanoDrop ND-1000 spectrophometer (Thermo Fisher Scientific, Waltham, MA, USA), and each sample was processed in triplicate for quantification of miR-34a and miR-34a target expression by quantitative real-time PCR (qRT-PCR). miR-708 levels were measured in the cerebellar samples only. The research met the criteria for Exemption 4 in terms of Human Subjects Research and was approved by the Institutional Review Board of the Massachusetts General Hospital.

Cell culture of proliferative human neural progenitors and differentiated neurons

Expandable human neuronal progenitor cells (hNPCs) from one unaffected male (GM08330, Coriell Institute for Medical Research Camden, NJ, USA) and one BD male (GM05224, Coriell Institute for Medical Research) were generated from iPSCs[31] (Madison *et al.*)[32] and cultured on poly-ornithine/laminin-coated six-well plates (BD Biosciences, San Jose, CA, USA) with neural expansion medium (70% Dulbecco's Modified Eagle Medium (DMEM) (Invitrogen, Carlsbad, CA, USA), 30% Ham's F-12 (Mediatech, Manassas, VA, USA) supplemented with B-27 (Invitrogen), 20 ng ml^{-1} each epidermal growth factor (Sigma-Aldrich, St Louis, MO, USA) and basic fibroblast growth factor (R&D Systems, Minneapolis, MN, USA). Terminal neural differentiation was achieved by plating NPCs at a seeding density of 4×10^4 cells per cm^2 on poly-ornithine/laminin-coated plates and culturing them for up to 8 weeks in differentiation medium DMEM/F12 (Invitrogen), Glutamax (Invitrogen) supplemented with B-27 and N2 (Invitrogen), 200 μM L-ascorbic acid (Sigma-Aldrich) and 100 μM dibutryl-cAMP (Sigma-Aldrich). Culture medium was replaced every 3–4 days during neural differentiation. Cell samples were collected by manual scraping, pelleted by centrifugation to remove culture medium, quickly frozen on dry ice and finally stored at − 80 °C.

Culture and transdifferentiation of human fibroblasts into induced neurons (iNs)

Human fibroblast lines were obtained from unrelated individuals aged ⩾18 years recruited from an outpatient BD clinic at Massachusetts General Hospital. Diagnosis of bipolar I disorder was confirmed by structured clinical interview (SCID-I)[33] conducted by a board-certified psychiatrist, which was supplemented by referring clinician report and medical records where available. SCID-I was completed to exclude any Axis I disorder other than nicotine abuse or dependence. All subjects signed written informed consent prior to study participation. The study protocol was approved by the Institutional Review Board of the Massachusetts General Hospital.

Fibroblast cultures were grown on substrates coated with 0.1% gelatin (Millipore, Billerica, MA, USA) in fibroblast media DMEM (Invitrogen) containing 10% fetal bovine serum (Gemini Bio-products, Calabasas, CA, USA), non-essential amino acids, glutamate and penicillin/streptomycin (Invitrogen). Lentiviral infection of human fibroblasts and conversion into iNs were performed as described in Yoo *et al.*,[34] with minor modifications. Briefly, miR-9/9*-124 together with NEUROD2, ASCL1 and MYT1L (kindly provided by the Crabtree Lab, Stanford University, Stanford, CA, USA) were expressed in human fibroblasts. Infected cells were then maintained in fibroblast media supplemented with 1 mM valproic acid (VPA, Sigma) for 3–4 days before selection with appropriate antibiotics in Neuronal Medium (NM, ScienCell, Carlsbad, CA, USA) supplemented with 1 mM VPA for 7 days. Three-to-4 days after antibiotic selection, cells were passaged onto poly-ornithine/laminin (20 μg ml^{-1}) coated 96-well plates and maintained in NM supplemented with 1 mM VPA for an additional 7 days, after which VPA was withdrawn for the remaining differentiation period. Media were changed every 3–4 days. Thirty-eight-to-40 days after the initial lentiviral transduction, cells were treated with RNA Protect Cell Reagent (Qiagen, Valencia, CA, USA). Then RNA extraction was performed using the miRNeasy Micro Kit (Qiagen) as per the manufacturer's instructions.

miRNA and mRNA qRT-PCR

The miRNeasy Mini Kit (Qiagen) was used for RNA extraction per the manufacturer's instructions. Quality and concentration of total RNA was assessed using a NanoDrop ND-1000 spectrophotometer (Thermo Fisher Scientific). For mature miRNA measurements, 10–20 ng of total RNA were reverse transcribed using the Taqman microRNA Reverse Transcription Kit (Life Technologies, Foster City, CA, USA), and the product was diluted 1:15 in RNAse-free water. Levels of mature miRNAs, as well as normalizers RNU44 and U6 snRNAs, were assayed in triplicates following qRT-PCR with the Taqman qRT-PCR assays (Life Technologies) and analyzed using the formula $C = 2^{Ctgeomean\ of\ normalizers}/2^{CtmiRNA}$. Both reverse transcription and qRT-PCR miRNA primers were part of the Taqman miRNA assays (Life Technologies). miR-34a expression was normalized to U6 and RNU44 expression to control for the total amount of RNA present in each sample. For mRNA measurements, 300 ng of RNA were reverse transcribed using the VILO cDNA Synthesis Kit (Invitrogen). The geometric mean of β-actin and 18S rRNA or 18S rRNA alone was used for normalization using the following formula: $C = 2^{Ctnormalizers}/2^{CtmRNA}$.

Bioinformatic prediction of miR-34a targets

To predict miR-34a targets, we used miRWalk database, http://www.umm.uni-heidelberg.de/apps/zmf/mirwalk/micrornapredictedtarget.html,[35] which allows a comparative analysis by eight prediction programs (DIANAmT, miRanda, miRDB, miRWalk, RNAhybrid, PICTAR, RNA22 and Targetscan).[36–42] Our search was restricted to miRNA-binding sites within the 3′ untranslated region (UTR), with a minimum seed length of seven nucleotides between the miR-34a sequence and its predicted targets. Because of performance differences between algorithms (that is, sensitivity and specificity in target prediction), we retained only targets that were predicted by at least four different programs. We then compared this list to the BD genome-wide association studies (GWAS) list (140 genes published in Sklar *et al.*[16]) and found 25 genes overlapping with both lists (see Table 1). For gene ontology analysis of miR-34a-predicted targets, we used Targetscan 6.2 (http://www.targetscan.org/) and miR-34 family-predicted targets were analyzed using DAVID Bioinformatics Resources 6.7 http://david.abcc.ncifcrf.gov/tools.jsp.[43] Gene ontology categories and disease enrichment were assayed (see Supplementary Tables S3–S7).

Western blotting

For western blotting analyses, frozen cell pellets were rapidly re-suspended in ice-cold radio-immunoprecipitation assay buffer 50 mM Tris-HCl (pH 8.0), 300 mM NaCl, 0.5% Igepal-630, 0.5% deoxycholic acid, 0.1% sodium dodecyl sulfate (SDS), 1 mM EDTA) supplemented with protease inhibitors (Complete Protease Inhibitor without EDTA, Roche Applied Science, Indianapolis, IN, USA) and phosphatase inhibitors (Phosphatase Inhibitor Cocktail A, Santa Cruz Biotechnology, Santa Cruz, CA, USA). One volume of 2× Laemmli buffer 100 mM Tris-HCl (pH 6.8), 4% SDS, 0.15% Bromophenol Blue, 20% glycerol, 200 mM β-mercaptoethanol) was added, and the extracts were boiled for 5 min. Protein concentration for each sample was determined using the Pierce BCA Protein Assay Kit (Thermo Fisher Scientific, Rockford, IL, USA). Equal amount of lysate for each sample was separated using SDS-polyacrylamide gel electrophoresis and transferred to a nitrocellulose membrane. After transfer, the membrane was blocked in TBST (Tris-buffered saline and 0.1% Tween 20) supplemented with 5% milk and probed with the indicated primary antibody at 4 °C overnight. After washing with TBST, the membrane was incubated with the appropriate horseradish peroxidase (HRP)-conjugated secondary antibody (Santa Cruz Biotechnology) and visualized using ECL reagents according to the manufacturer's guidelines (Pierce, Thermo Fisher Scientific). Quantification of each tested antigen was performed by densitometry analysis of three independent biological replicates.

Immunocytochemistry

Indirect immunofluorescence detection of antigens was carried out in hNPCs and differentiated neurons cultured on poly-ornithine/laminin-

Table 1. List of the 25 predicted miR-34a targets overlapping with BD GWAS and with a score > 4

Gene	*Algorithm*	*DIANAmT*	*miRanda*	*miRDB*	*miRWalk*	*RNAhybrid*	*PICTAR*	*RNA22*	*Targetscan*	*SUM*
1	*ANK3*	1	1	1	1	1	1	1	1	8
2	*CACNB3*	1	1	1	1	1	0	1	1	7
3	*PACS1*	1	1	1	1	1	0	1	1	7
4	*DPP3*	1	1	1	1	1	0	0	1	6
5	*LMBR1L*	1	1	0	1	0	1	1	1	6
6	*SPTBN2*	1	1	0	1	1	1	0	1	6
7	*KLC2*	1	1	0	1	0	0	1	1	5
8	*C2orf55*	1	1	0	1	1	0	0	1	5
9	*FUT1*	1	1	1	1	0	0	0	1	5
10	*LBA1*	1	1	0	1	0	1	0	1	5
11	*MGAT4A*	1	1	1	1	0	0	0	1	5
12	*RAB1B*	1	1	0	1	0	1	0	1	5
13	*SH3PXD2A*	1	1	1	1	0	0	0	1	5
14	*CACNA1C*	1	1	0	1	0	0	0	1	4
15	*BBS1*	1	1	0	1	0	0	0	1	4
16	*CNNM4*	1	1	0	1	0	0	0	1	4
17	*DDN*	1	1	0	1	0	0	0	1	4
18	*LMAN2L*	1	0	0	1	1	0	0	1	4
19	*MRPL30*	1	1	0	1	0	0	0	1	4
20	*ODZ4*	1	1	0	1	0	0	0	1	4
21	*PPM1M*	1	0	0	1	0	1	0	1	4
22	*PRKAG1*	1	1	0	1	0	0	0	1	4
23	*RIN1*	1	1	0	1	0	0	0	1	4
24	*SEMA3G*	1	1	0	0	0	1	0	1	4
25	*ZMIZ1*	1	1	0	1	0	0	0	1	4

Abbreviations: BD, bipolar disorder; GWAS, genome-wide association study. List of predicted miR-34a targets was generated using the miRWalk database that considers eight different target prediction programs. Only targets predicted by at least four programs and overlapping with the BD GWAS list (140 genes published by Sklar *et al.*[16]) were retained. Color code: green = predicted and scored = 1, red = not predicted and scored = 0, and last column showed the final score.

coated 96-well plates (Costar, Cambridge, MA, USA) or similarly coated 24-well plates with glass coverslips. Cells were first washed twice with phosphate-buffered saline (PBS) and fixed for 30 min at room temperature with 4% paraformaldehyde in PBS. After fixation, cells were washed twice with PBS, permeabilized with PBS-T (PBS and 0.25% Triton X-100) for 20 min, blocked in blocking solution (5% normal serum in PBS-T) for 30 min and finally incubated overnight at 4 °C with the first primary antibody in blocking solution. Next day, cells were washed with PBS and incubated for 2 h at room temperature in the appropriate fluorophore-conjugated secondary antibody solution (Alexa 488- or Alexa 594-conjugated secondary antibody (Molecular Probes, Invitrogen, Carlsbad, CA, USA) in blocking solution). After washes with PBS, cells were incubated again overnight in primary antibody solution for the second antigen, and the procedure for conjugation of the fluorophore-conjugated secondary antibody was repeated as above. Finally, cell nuclei were counterstained with 4′,6-diamidino-2-phenylindole and washed twice before imaging using a fully automated epifluorescence microscope equipped with a ×20 Fluor objective and a Photometrics CoolSNAP HQ 12-bits digital interline CCD camera (ImageXpress Micro, Molecular Devices, Sunnyvale, CA, USA). For each condition, four wells were imaged with six different sites per well. Cells cultured on glass coverslips were mounted on glass slide with Prolong antifade reagent (Invitrogen) and imaged using a Zeiss Axio Observer Z1 inverted microscope, Carl Zeiss, Göttingen, Germany.

Antibodies

The rabbit anti-ANK3 (Ankyrin-G; sc-28561), the goat anti-SOX1 (sc-17318) and the HRP-conjugated secondary antibodies were from Santa Cruz Biotechnology. The chicken anti-green fluorescent protein (A10262) and rat anti-mCherry (M11217) were from Life Technologies. The mouse anti-PSD95 (Clone K28/43, 75-028) was from NeuroMab (UC Davis, CA, USA), the rabbit anti-SOX2 (ab59776) from Abcam (Cambridge, MA, USA) and the rabbit anti-Tuj1 (PRB-435P) from Covance (Richmond, CA, USA). The rabbit anti-CACNB3 was purchased from LifeSpan BioSciences (Seattle, WA, USA). The mouse monoclonals anti-Synaptophysin (S5768) and the anti-β-actin (A1978) were from Sigma. Finally, the rabbit anti-Musashi (AB5977) was from Millipore, and the mouse anti-Synapsin 1 (106 001) as well as guinea pig anti-MAP2 (188 004) were purchased from Synaptic Systems (Gottingen, Germany).

Luciferase reporter constructs

The 3′UTRs of *CACNB3* (1116 bp, refseq. NM_000725.3), *DDN* (1698 bp, refseq. NM_015086.1) and *KLC2* (964 bp, refseq. NM_001134775.1) were PCR amplified from the human brain cDNA (Invitrogen) and cloned downstream of the phosphoglycerate kinase I promoter-driven luciferase reporter gene luc2 expression in the pmirGLO Dual-Luciferase miRNA Target Expression Vector (Promega, Madison, WI, USA). The 3′UTR of *ANK3* (refseq. NM_001149.3), *CACNA1C* (refseq. NM_199460.2) and *SYT1* (refseq. NM_005639) were cloned by GeneCopoeia downstream of the SV40 promoter-driven secreted Gaussia luciferase (GLuc) reporter gene in a firefly/Renilla Duo-Luciferase reporter vector (pEZX-MT01). For miR-34a target validation, HEK293T cells were seeded at a density of 10^4 cells per well in a 96-well plate and grown for 24 h before transient transfection with 20–40 ng of each dual luciferase reporter construct and 30 nM of pre-miR-34a or pre-miR-Neg (Ambion, Austin, TX, USA) using Lipofectamine 2000 (Invitrogen). Luciferase activities were measured 48 h after transfection using the Dual Glo Luciferase Assay System (no. E2920, Promega) or the Luc-Pair miR Luciferase Assay Kit (LPFR-M030, GeneCopoeia, Rockville, MD, USA) depending on the luciferase reporter constructs. Efficiency of transfection was normalized using the Renilla luciferase activity.

Overexpression and suppression of miR-34a expression

For overexpression of miR-34a, hNPCs (unaffected male, derived from GM08330 iPSCs) were seeded at a density of 1.5×10^5 cells per well of a 12-well plate and transduced with the human Lenti-miR-34a or Lenti-miR-Ctrl expression system (Biosettia, San Diego, CA, USA) 2 h after plating. The titer of the virus was ~ 1×10^7 infection units per ml, and cells were transduced with a multiplicity of infection equal to 33. Each miRNA precursor in the lentiviral vector was cloned from its native context, including its flanking and stem-loop precursor sequence within the intron of human EF1α promoter region. This ensured that each miRNA was properly expressed and processed and would function similarly to its endogenous form. miR-Ctrl has no DNA sequence inserted into the EF1α intron. A complete

medium change was performed after 7 h of transduction. Then selection of NPCs expressing miR-34a or miR-Ctrl started after 3 days of transduction for 10 days with the medium containing 1 μg ml^{-1} puromycin (Sigma). hNPCs stably expressing miR-34a and miR-Ctrl were expanded and seeded for subsequent differentiation.

For suppression of miR-34a expression, hNPCs (unaffected male, derived from GM08330 iPSCs) were transfected after 12 days of differentiation with either a construct expressing an anti-miR-34a sequence (GeneCopoeia, HmiR-AN0440-AM03-B) or a control scrambled sequence (GeneCopoeia, CmiR-AN0001-AM03). As both constructs co-expressed mCherry as a reporter gene, for these experiments the 2-day transfected cells were fixed cells and immunostained for mCherry to allow complete visualization of the cells expressing the anti-miR constructs. The Sholl analysis was done as described above for the miR-34a overexpressing hNPCs. To assess the effect of the anti-miR-34a expression on target mRNAs, transfected cells were selected for 2 days using an antibiotic selection with hygromycin B at 200μg ml^{-1}.

Neuronal morphology measurement

For the analysis of the miR-Ctrl and miR-34a overexpressing hNPCs, the cells were seeded on glass coverslips at a density of 100 000 cells per well and differentiated as neurons. To measure the arbor complexity of the cells in both conditions after 3 weeks of differentiation, the cells were transfected at 19 days for 30 min with Lipofectamine 2000 and a plasmid encoding a membrane-bound form of enhanced green fluorescent protein (Addgene, Plasmid 14757, Cambridge, MA, USA). Forty-eight hours after transfection, the cells were then fixed and immunostained for green fluorescent protein to enhance the signal and allow the complete visualization of the neuronal morphology. A total of 40 transfected neurons per condition from five biological replicates were captured using a Zeiss Axio Observer microscope and a ×20 objective. The Sholl analysis was performed by superimposing concentric equidistant (10 μm) circles around the neuronal soma using the Adobe Illustrator CS (Adobe Systems, San Jose, CA, USA) and counting the number of intersecting branches along the circumference of each circle. In a separate experiment, the effect of inhibiting miR-34a on the arbor complexity of differentiating hNPCs transfected with either the anti-miR-34a sequence (GeneCopoeia, HmiR-AN0440-AM03-B) or a control scrambled sequence (GeneCopoeia, CmiR-AN0001-AM03) was observed. As both plasmids co-expressed mCherry as a reporter gene, for these experiments the fixed cells were then immunostained for mCherry to allow complete visualization of transfected cells, and Sholl analysis was done as described above for the miR-34a overexpressing hNPCs.

Multiplexed mRNA profiling assay using the NanoString technology

Using a multiplexed, digital, mRNA profiling assay based on NanoString single-molecule, direct mRNA counting technology, we constructed a 131 unique gene probe set covering 18 genes located within the major loci identified to date through GWAS as being associated with BD susceptibility, as well as an additional 113 unique genes implicated in neurodevelopment, functionally connected to ankyrin and ion channels, as well as in schizophrenia given the growing evidence for cross-disorder, shared genetic etiology by GWAS (Supplementary Table S8).[23] Data were normalized to the geometric mean of 13 selected reference genes (*CBX3*, *DDX24*, *EEF1B2*, *NUDCD3*, *CEP170*, *NACAP1*, *LOC552889*, *ESD*, *MEA1*, *FAM162A*, *SEPT9*, *HP1BP3*, *RPRD1A*) selected for flat expression signature in brain array data.

Data analysis and computational methods

Data are expressed as means ± s.e.m. Statistical analysis was performed using the GraphPad Prism6 (GraphPad Software, Inc., San Diego, CA, USA). Data distribution and normality were assayed using the Shapiro–Wilk or D'Agostino and Pearson omnibus normality tests. The Student two-tailed *t*-test (one sample or two sample) or two-tailed Mann–Whitney test was used for statistical comparison between the two groups (based on normality), and analysis of variance with the Newman–Keuls Multiple Comparison Test was used for comparisons between more than two groups. Two-way analysis of variance was used to estimate the effects of diagnosis and developmental stage in iPSC-generated neurons, as well as quantify western blotting experiments. *Post hoc* comparisons between two means were conducted using the Bonferroni correction. The Spearman's or Pearson's correlation coefficients (based on normality) were applied for comparing correlations in postmortem data in which one BD sample was excluded as outlier based on Grubb's test in miR-34a; two controls and one bipolar sample were excluded for very low normalizer expression for *ANK3* and *CACNB3* measurements. Student's *t*-test for unpaired data with equal variance was applied for the Sholl analyses. In order to assess whether there was evidence within the NanoString profiles for common molecular pathways being affected by miR-34a overexpression, as the selection of 131 genes for inclusion in the NanoString probe set was purposely biased to cover genes implicated by neuropsychiatric genetics and ion channels, we deemed consideration of enrichment with Gene Ontology or related categories inappropriate. As an alternative computational approach to the systems-based modeling of the differential gene expression data, we determined whether there were statistically significant properties of the protein–protein interaction network among the validated miR-34a-target genes using VisANT 4.0 (http://visant.bu.edu) and/or the proteins encoded by the differentially expressed genes using DAPPLE v2.0 (Disease Association Protein-Protein Link Evaluator) (Figure 4).

RESULTS

miR-34a expression is increased in the cerebellum of BD patients and in cellular models derived from BD patients

Given the known influences of mood stabilizers on miR-34a levels and its potential role in neuronal maturation and plasticity, we decided to investigate the link between miR-34a and BD. Interestingly, two recent studies,[44,45] as well as unpublished data (SJH, manuscript in preparation), reported decreased expression of the two putative miR-34a targets *ANK3* and *CACNA1C* in the cerebellum of BD individuals. Based on these findings and emerging literature linking the cerebellum with BD,[44–53] we hypothesized that miR-34a could be dysregulated in the cerebellum of BD patients. To test this hypothesis, we measured the miR-34a expression in postmortem human brain samples from the cerebellum. We observed a significant increase in miR-34a levels in the cerebellum of BD patients ($N = 29$) relative to healthy controls ($N = 34$) (Figure 1a), whereas no differences were seen in prefrontal cortex (PFC) or anterior cingulate cortex (Supplementary Figures S1A and B). In contrast to this BD and brain region-specific difference in the miR-34a expression, based on the recent identification by GWAS of a new susceptibility locus within the first intron of *ODZ4* where miR-708 is encoded,[16] which is predicted to target both *ODZ4* itself and *CACNA1C*, the latter of which has shown multiple associations with neuropsychiatric disorders,[54] we also measured miR-708 in the same cerebellum samples from BD individuals (Supplementary Figure S1C) but did not see any differences compared with the healthy controls. Therefore we did not pursue the investigation of miR-708 targets and focused our study on miR-34a.

As mood stabilizers have been shown to affect miR-34a expression,[24,25,55] we segregated BD individuals based on whether or not they were under treatment with mood stabilizer medications (Figure 1b) and observed a significant increase in miR-34a expression only in BD individuals without treatment, suggesting a potential normalizing effect on miR-34a expression following treatment (Figure 1b). Interestingly, a significant correlation between the age of onset of the disease and psychotic symptoms on miR-34a levels was observed (Supplementary Figures S1D and E), without evidence for interaction of other confounding factors (Supplementary Table S1, Supplementary Figures S1F–H). Although sex differences did not significantly affect miR-34a levels in healthy control samples (data not shown), there was a more robust increase in miR-34a in female BD patients (Supplementary Figure S1I).

Finally, to provide orthogonal validation of our findings in postmortem brain samples, and escape the known limitations of postmortem brain molecular analysis that until development of reprogramming technology have been the mainstay of functional analyses of molecular and cellular phenotypes in BD, we assessed the expression of miR-34a upon differentiation of human iPSC-

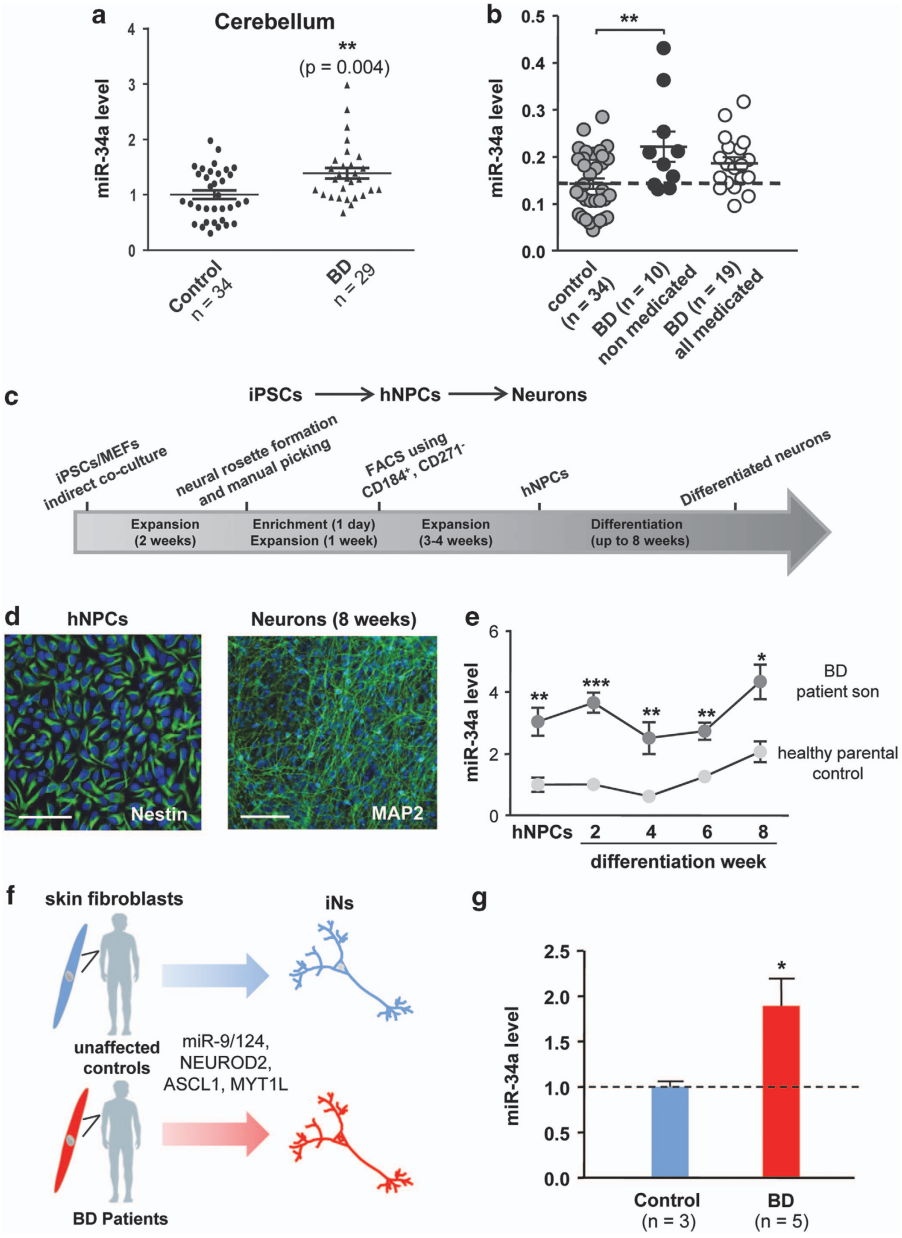

Figure 1. miR-34a expression is increased in the cerebellum of bipolar disorder (BD) patients and in patient-derived cellular models of BD. (**a**) Mean ± s.e.m. miR-34a levels depicted as fold change relative to controls. $N = 34$ control and 29 BD cerebellar samples. $^{**}P < 0.01$ compared with control conditions, based on a two-tailed, one-sample *t*-test. (**b**) Mean ± s.e.m. miR-34a levels in the cerebellum of controls ($N = 34$) and BD patients segregated into medicated ($N = 19$) and non-medicated ($N = 10$). $^{**}P < 0.01$ based on analysis of variance with Tukey's Multiple Comparison Test. (**c**) Schematic of the neuronal differentiation process from induced pluripotent stem cells (iPSCs) to 8-week differentiated neurons. (**d**) Immunostaining of Nestin in human neuronal progenitor cells (hNPCs) and MAP2 in 8-week differentiated neurons, scale bar = 50 μm. (**e**) Graphs showing relative miR-34a expression in hNPCs and differentiated neurons of a healthy control individual (light grey circles) and a BD patient (dark grey circles). Data are shown as fold change relative to miR-34a level at the hNPC stage. Asterisks over data depict statistical significance based on a two-tailed *t*-test ($^{*}P < 0.05$, $^{**}P < 0.01$, $^{***}P < 0.001$). (**f**) Schematic of the generation of induced neurons (iNs). (**g**) miR-34a expression in iNs from three control and five BD subjects. The graph shows mean ± s.e.m. miR-34a expression relative to control iNs. miR-34a expression was normalized to U6 and RNU44 expression, which control for the total amount of RNA present in each sample. $^{*}P < 0.05$ compared with control conditions, based on a two-tailed, one-sample *t*-test. FACS, fluorescence-activated cell sorter; MEF, mouse embryonic fibroblast.

derived NPCs (hNPCs) generated from one BD patient (Madison *et al.*)[32] and their healthy parent (father) as a control.[31] The level of neuronal differentiation was evaluated by measuring multiple differentiation markers at different developmental stages (Figures 1c and d and Supplementary Figures S2A–F). Of note, both hNPC lines express the neural progenitor marker Nestin at similar level (Supplementary Figure S2G). We found that miR-34a was expressed at low levels in hNPCs and was modestly upregulated upon differentiation (Figure 1e). Unexpectedly, BD-derived hNPCs and neurons expressed significantly more miR-34a levels in comparison with the wild-type unaffected relative control samples. To complement these iPSC-based findings with a

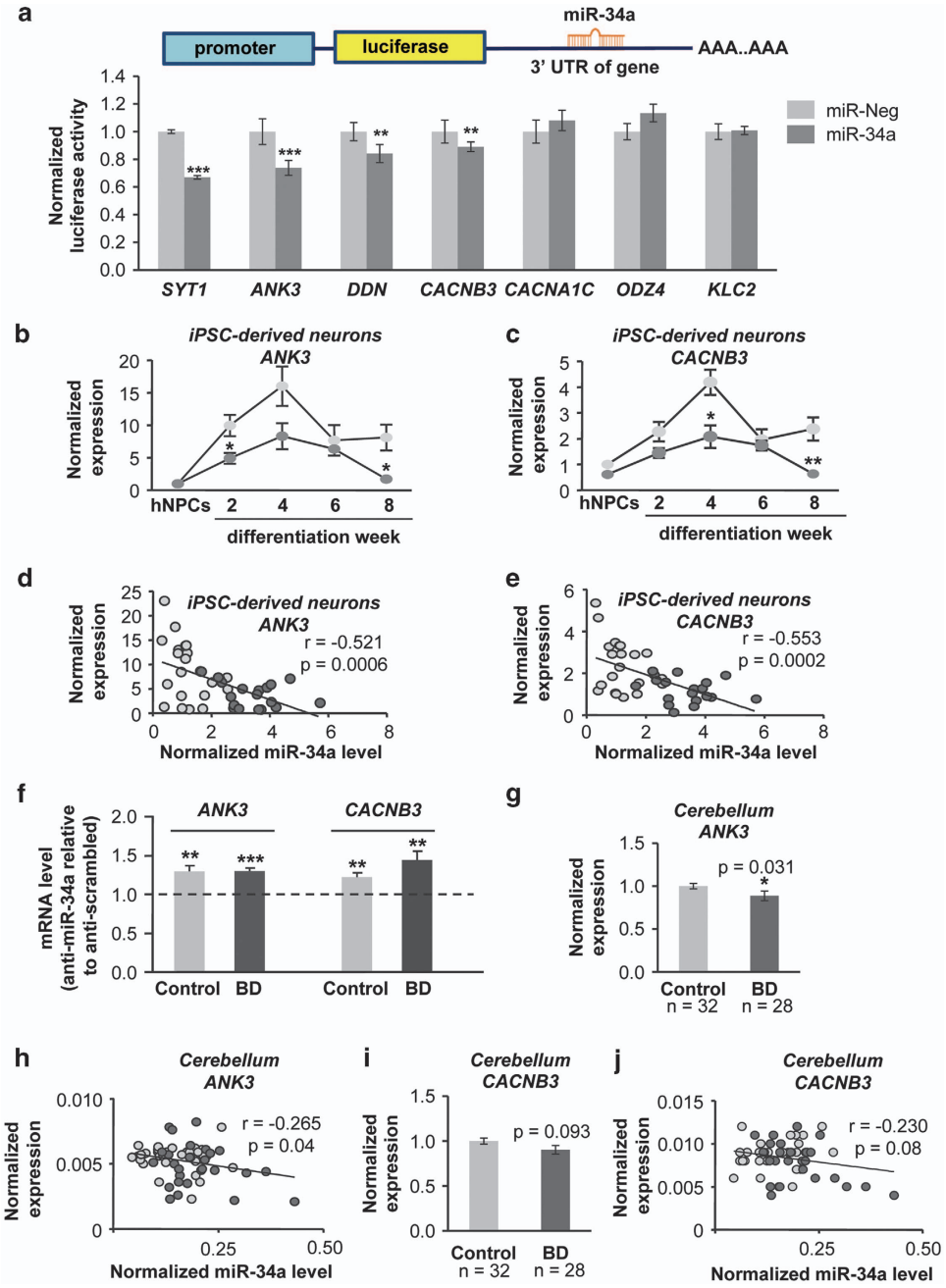

Figure 2. Bipolar disorder (BD)-related genes differentially expressed during differentiation of human induced pluripotent stem cell (iPSC)-derived neuronal progenitors are targets of miR-34a. (**a**) Upper: Schematic of luciferase assay. The interaction of a putative target with miR-34a is shown. Lower: Results from luciferase reporter gene assays in HEK293T transfected with either a non-targeting control having no sequence homology to the human (miR-Neg—light grey bars) or miR-34a mimics (dark grey bars). Data are shown as fold change relative to miR-Neg treatment. $^{**}P < 0.01$, $^{***}P < 0.001$ compared with miR-Neg treatment, based on a two-tailed, one-sample *t*-test. (**b**–**e**) Expression (**b**, **c**) and correlation (**d**, **e**) data relative to miR-34a expression of the two validated miR-34a targets *ANK3* (**b**, **d**) and *CACNB3* (**c**, **e**) in control (light grey bars) and BD (dark grey bars) iPSC-derived neuronal progenitor cells (NPCs)/neurons. Data are shown as fold change relative to miR-34a level at human NPC (hNPC) stage. Asterisks over data depict statistical significance based on a two-tailed *t*-test ($^{*}P < 0.05$, $^{**}P < 0.01$, $^{***}P < 0.001$). Spearman correlation coefficients (*r*) and *P*-values (two-tailed) are shown. (**f**) Control (light grey bars) and BD patient (dark grey bars) iPSC-derived NPCs were transfected with either an anti-miR-scrambled or anti-miR-34a construct designed to trap endogenous miR-34a and differentiated for 2 weeks. Data show expression of the two validated miR-34a targets *ANK3* and *CACNB3* expressed as the ratio of anti-miR34a to anti-miR-scrambled. Asterisks over data depict statistical significance based on a two-tailed *t*-test ($^{**}P < 0.01$, $^{***}P < 0.001$). (**g**–**j**) Expression (**g**–**i**) and correlation (**h**–**j**) data relative to miR-34a expression of *ANK3* (**g**, **h**) and *CACNB3* (**i**, **j**) in the cerebellum of controls (light grey bar, $N = 32$) and BD patients (dark grey bar, $N = 28$). Asterisk and *P*-value depicted in panels (**g**) and (**i**) are based on two-tailed, Mann–Whitney test ($^{*}P < 0.05$). Pearson correlation coefficients (*r*) and *P*-values (two-tailed) are shown.

different, and a larger, set of control and patient-derived cellular models of BD, we turned to the use of newly developed, direct reprogramming methods to create iNs.[34] As shown in Figure 1f, iNs were generated through the transdifferentiation of human fibroblasts derived from BD patients and psychiatrically screened healthy controls. Similar to our findings comparing the healthy parental iPSC-derived neurons to those of the BD patient son, we found a significant increase in miR-34a expression in iNs derived from BD patients compared with healthy control cultures (Figure 1g). Taken together, these postmortem and cellular data, which have allowed the analysis of the molecular profiles of live human neurons generated using two different reprogramming approaches, suggest that miR-34a expression is dysregulated in the context of BD.

miR-34a targets BD risk genes *ANK3*, *CACNB3*, and *DDN*

Given the observed upregulation of miR-34a expression, we next aimed to identify miR-34a targets potentially relevant to the pathogenesis of BD through consideration of genetic risk factors identified by recent, large-scale, BD GWAS by the Psychiatric GWAS Consortium.[16] Using *in silico* analysis,[35] we identified 25 overlapping miR-34a targets predicted by at least four different algorithms (Table 1).

Based on their known brain expression patterns and potential biological relevance in the context of neuropsychiatric disorders, we elected to follow-up 6 of the 25 putative miR-34a targets that overlap with genes within the BD GWAS loci: *ANK3*, *CACNA1C*, *CACNB3*, *ODZ4*, *DDN*, and *KLC2*.[16,44,45,56,57] To further explore the putative miR-34a targets, we first checked the predicted binding site between the target mRNA and miR-34a using TargetScan (Supplementary Table S2). Then to experimentally validate the predicted miR-34a targets, we needed to test whether the interaction sites between miR-34a and the mRNA targets are functional.[58,59] Luciferase reporter assays revealed that miR-34a overexpression was capable of targeting and silencing the BD risk genes *ANK3*, *DDN* and *CACNB3* along with the previously shown target gene *SYT1*[27] but had no effect on the 3′UTRs of *CACNA1C*, *ODZ4* and *KLC2* (Figure 2a). In addition, global analysis of miR-34a-predicted targets showed enrichment of molecular networks related to neuronal development, differentiation and synaptic plasticity, as well as gene sets implicated in neurodevelopmental disorders (Supplementary Tables S3–S7[43]). Taken together, these results validate three genes implicated in BD risk as miR-34a targets and suggest that miR-34a may function to regulate an interacting molecular network important to BD pathogenesis through effects on neurodevelopment.

To further investigate the functional consequence of altering miR-34a expression throughout early neurodevelopment, we next assessed the expression of putative miR-34a targets upon differentiation of iPSC-derived NPCs (hNPCs). Among the six putative miR-34a targets, mRNA levels of four (*ANK3*, *CACNB3*, *ODZ4* and *KLC2*) were gradually increased until 4 weeks of differentiation, and then partially downregulated by 8 weeks, whereas *CACNA1C* mRNA expression gradually increased during the 8 weeks of differentiation (Figures 2b and c and Supplementary Figure S3). *DDN* was not expressed in either hNPCs or differentiated neurons preventing its further analysis (data not shown). As we observed an increase of miR-34a expression in BD patient-derived cellular models, we expected that the expression of *bona fide* miR-34a targets would be decreased. Indeed, miR-34a-validated targets were significantly downregulated in iPSC-derived neurons from BD individuals (Figures 2b–e).

As a further test of the correlation between miR-34a levels and its putative endogenous target genes in human iPSC-derived neurons, we used a miRNA inhibitor construct (anti-miR-34a) designed through its sequence complementarity to selectively trap endogenous miR-34a thereby preventing miR-34a association with its target genes along with a non-targeted control inhibitor construct (anti-scrambled). As a result of inhibiting endogenous miR-34a, expression of a miR-34a inhibitor construct is expected to reduce the effects of miR-34a on mRNA stability and translational suppression resulting in an increase in target gene expression. The anti-miR-34a and anti-scrambled constructs were expressed in hNPCs from both the healthy control and BD son patient. After 2 weeks of differentiation, as shown in Figure 2f, as predicted, expression of the anti-miR34a construct increased the expression of both *ANK3* and *CACNB3* in both the control and BD patient iPSC-derived neurons.

Finally, further emphasizing the reciprocally related expression of miR-34a and its putative targets, given the upregulation of miR-34a in the postmortem cerebellum of BD patients, we observed similarly decreased *ANK3* and *CACNB3* mRNA levels, which were also negatively correlated with miR-34a expression (Figures 2g–j). Of note, the limited amount of RNA collected from iNs did not allow further investigation of the correlation of targets to the level of miR-34a expression. Taken together, these observations further support the validation of the two miR-34a targets *ANK3* and *CACNB3*.

miR-34a dysregulation alters differentiation of human iPSC-derived neurons

As a complement to the anti-miR-34a studies that showed an elevation of putative miR-34a target genes, to examine the effect of increasing miR-34a levels on target gene expression and neurodevelopment we stably overexpressed miR-34a in hNPCs from a healthy control subject and differentiated them for up to 8 weeks (Figure 3a). miR-34a overexpression decreased the levels of *ANK3* and *CACNB3* as observed in differentiated neurons relative to a negative control miRNA construct (miR-Ctrl) especially in the latest stages of differentiation (Figures 3b–e). Changes in target expression were not seen at the hNPC stage (Figures 3d–e), again pointing to a temporal dependency of the neurodevelopmental regulation of miR-34a targets. To further investigate how miR-34a upregulation observed in BD patient samples could affect pathophysiology, we assessed neuronal differentiation in miR-Ctrl and miR-34a-overexpressing cells with a panel of biochemical markers (Figures 3d and e). Consistent with a blockade of neuronal differentiation, miR-34a overexpression delayed the expression of the presynaptic and postsynaptic neuronal markers SYP, SYN1 and PSD-95 over the neurodevelopmental time course (Figures 3d and e). In agreement with these findings, a similar phenotype was observed in the 2-week differentiated neurons from the BD line in which miR-34a expression was previously found to be upregulated (Figure 3d). Of note, SYP and CACNB3 are not expressed at this stage of differentiation (Figure 3d). Moreover, ectopic overexpression of miR-34a and inhibition of endogenous miR-34a using an anti-miR-34a strategy altered neuronal morphology (Figures 3f–h), resulting in a significant reduction or increase of dendritic length and branch number when miR-34a expression was increased or decreased, respectively (Figures 3g and h). These results are highly reminiscent of those observed by Agostini *et al.*[26] in mouse cortical neurons revealing with this the first demonstration in human neurons of an evolutionarily conserved function of miR-34a in the regulation of dendritic morphology.

Having demonstrated that manipulation of miR-34a expression in human iPSC-derived NPCs causes aberrant expression of synaptic proteins and the establishment of morphologically complex neurons, we sought next to determine the effects of miR-34a expression on a broader set of 18 genes implicated in neuropsychiatric disorders and neurodevelopment by recent GWAS of BD, as well as *SYP* and *SYN1* as controls based upon our western blotting data showing synaptic dysregulation (Figure 4, Supplementary Figures S4–S6, Supplementary Tables S8–S10 and Supplementary Text). Using a multiplexed, digital,

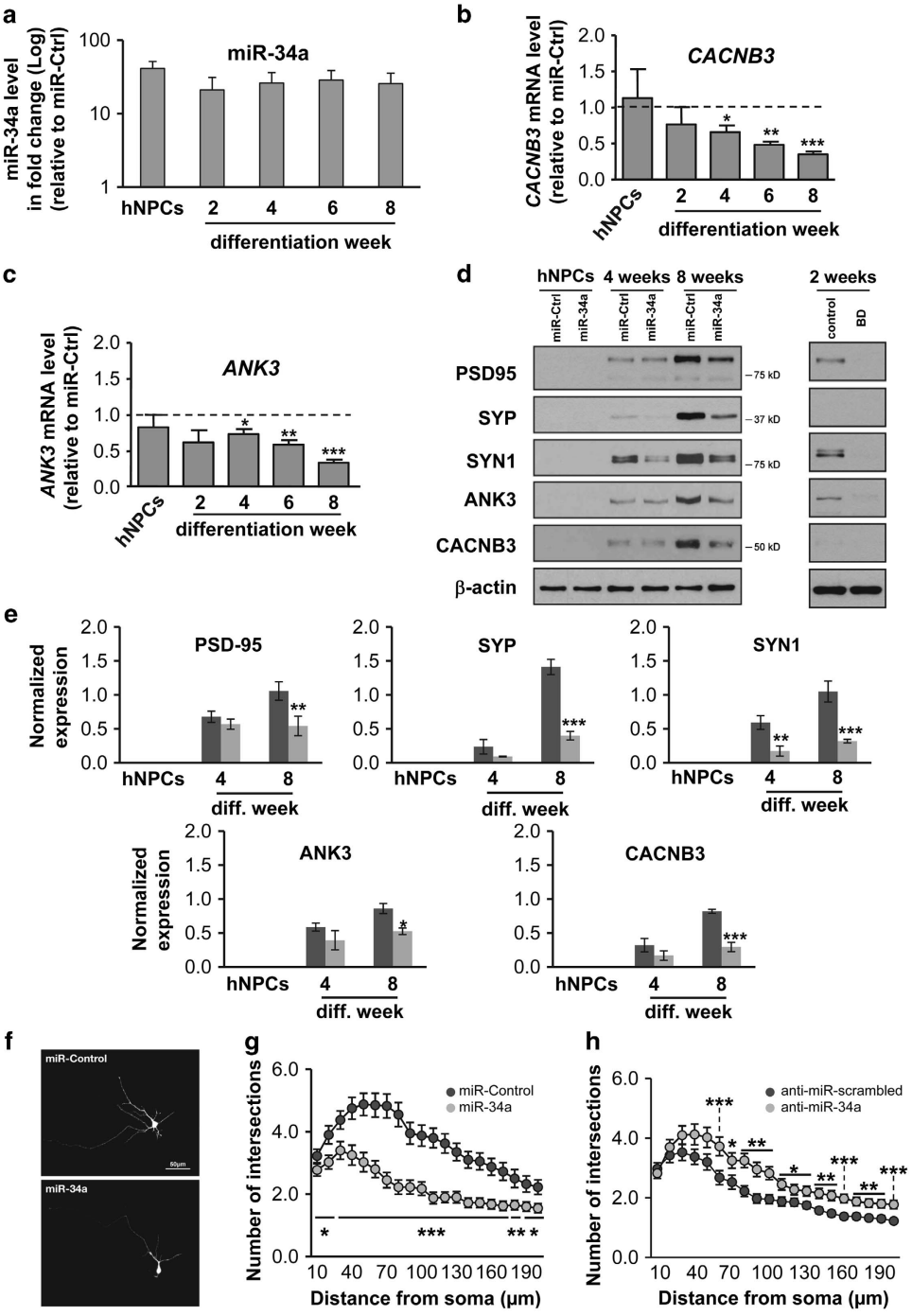

mRNA profiling assay based upon NanoString single-molecule, direct mRNA counting technology, among the genes we tested, miR-34a overexpression significantly affected the expression of nine genes (*SYNE1*, *CACNA1C*, *CACNB3*, *SYN1*, *TNR*, *SYT12*, *SYP*, *ANK3*, *TMEM110*), with *ODZ4* and *ITIH4* close to having a significant difference (Figure 4a and Supplementary Figure S4).

To gain more insight into target genes either directly or indirectly affected by miR-34a overexpression over a temporally defined time course of human neurodevelopment, the miR-Ctrl and miR-34a overexpression lines were differentiated for 8 weeks. Total RNA samples collected at $t = 0$, 2, 4 and 8 weeks in duplicate and subjected to the NanoString assay with a probe set consisting of a total of 131 genes, and the data were merged with that from the $t = 6$ weeks sets that were done in triplicates (Supplementary Tables S8 and S9). Using a cutoff of a change $> \pm 1.5$-fold with miR-34a overexpression compared with the matched miR-Ctrl control, along with the requirement that at least two of the replicates showed concordant results for the particular time period, a total of 70 transcripts (53%) were identified at one more time point over the neurodevelopmental time course as showing differential expression (Supplementary Table S10). Of these 70 transcripts, 14 were within one of the BD-associated GWAS loci, including both *ANK3* and *CACNB3*, which replicates with digital mRNA counting assay, the qRT-PCR results and western blotting

Figure 3. Ectopic expression of miR-34a decreases CACNB3 and ANK3 expression and affects neuronal differentiation and morphology of human induced pluripotent stem cell-derived neurons. (**a**) Human neuronal progenitor cells (hNPCs) were transduced with either miR-Ctrl or miR-34a lentiviral constructs and differentiated for 8 weeks. Data show expression of miR-34a shown as fold change relative to the transcript level at the initial hNPC stage. (**b**, **c**) Follow-up of the two validated miR-34a targets *ANK3* and *CACNB3* at the transcriptional level in miR-Ctrl and miR-34a overexpressing hNPCs and differentiated neurons. Data are shown as fold change relative to the transcript of interest at hNPC stage and normalized to the transcript level in miR-Ctrl conditions. Data are mean ± s.e.m. from three independent experiments. $*P < 0.05$, $**P < 0.01$, $***P < 0.001$ compared with miR-Ctrl treatment, based on a two-tailed, one-sample *t*-test. (**d**) PSD95, Synaptophysin (SYP), Synapsin-1 (SYN1), ANK3 and CACNB3 western blotting results on hNPCs, 4- and 8-week differentiated neurons overexpressing either miR-Ctrl or miR-34a (left panel) or 2-week differentiated control and BD neurons (right panel). β-Actin was used as an internal standard. (**e**) Quantification of western blotting data in panel (**d**) by densitometric analysis. The bars show the mean ± s.e.m. ratio of the protein of interest and β-actin signals, as evaluated by densitometric analysis of three independent biological replicates. $*P < 0.05$, $**P < 0.01$, $***P < 0.001$ compared with miR-Ctrl treatment, based on a two-way analysis of variance using the Bonferroni's correction as *post hoc* comparisons between two means. (**f**) Image-based analysis of the effect of miR-34a overexpression on the morphology of hNPCs after 3 weeks of differentiation with sparse transfection with membrane-targeted green fluorescent protein for 2 days, scale bar = 50 μm. (**g**, **h**) Graph showing the number of branches in function of the soma distance in panel (**g**), 3-week differentiated neurons overexpressing miR-Ctrl (dark grey circles) and miR-34a (light grey circles) or in panel (**h**), 2-week differentiated neurons expressing anti-miR-scrambled control (dark grey circles) and anti-miR-34a (light grey circles). Twelve-day differentiated cells were transfected with anti-miR constructs for 2 days. As both constructs co-expressed mCherry as a reporter gene, cells expressing the anti-miR constructs were immunostained for mCherry. For each condition, a total of 40 neurons were imaged and quantified using classical Sholl analysis. $*P < 0.05$, $**P < 0.01$, $***P < 0.001$ compared with miR-Ctrl treatment (**g**) or anti-miR-scrambled (**h**), based on a two-tailed *t*-test.

results shown in Figure 3. These 14 transcripts correspond to a frequency 78% of the 18 BD candidate genes assayed. Of the other non-BD candidate genes affected in the probe set, there were 56 genes corresponding to a frequency 49.6% of the total of the 113 non-BD candidate genes. Comparing these frequencies (77.8% BD genes vs 49.6% non-BD genes) represents a statistically significant greater enrichment of affected BD candidate genes than that expected by chance ($P < 0.05$; two-tailed, Fisher's exact test) (Supplementary Figure S5). In support of the notion that miR-34a targets a molecular network of inter-related proteins critical to neurodevelopment, analysis of protein–protein interactions among these newly validated (ANK3, CACNB3, DDN), previously validated (SYN1) targets and genes implicated by neuropsychiatric genetics[16,19,23] revealed a highly connected interaction network (Figure 4b and Supplementary Figure S6; See Supplementary Text for details). Together, these findings support the hypothesis that elevation of miR-34a levels coordinately affects functionally connected pathways important for brain development and that dysregulation of miR-34a may be sufficient to influence the expression of multiple candidate BD susceptibility genes and genes critical to human neurodevelopment.

DISCUSSION

Despite the emerging knowledge on the importance of miRNAs in brain function and disease, very little is known about the role of miRNAs in BD. Here we show that miR-34a is upregulated in postmortem BD brain and in two different patient-derived cellular models of BD and is predicted to target multiple genes implicated in the etiology of BD through recent GWAS studies.[16,30] In addition, we validate ANK3, CACNB3 and DDN as novel targets of miR-34a and implicate a molecular network of miR-34a targets. Finally, we demonstrate using human iPSC-derived neuronal cultures that miR-34a expression is negatively correlated to that of ANK3 and CACNB3 and impairs neuronal differentiation and morphology. In this context, our finding that the expression of an anti-miR-34a construct that traps endogenous miR-34a is sufficient to enhance dendritogenesis is particularly intriguing as it provides evidence that levels of one or more miR-34a target genes are rate-limiting for dendritic elaboration in human neurons.

Although our study is the first to show that miR-34a inhibits neuronal differentiation of human neurons, previous studies in animal models have described the effects of miR-34a on neural stem cells[60] and neuronal progenitors,[61] as well as on dendritic outgrowth and synaptic structure of neurons in culture.[26] Taken together with our results, these studies suggest that, although miR-34a inhibits neuronal maturation and synaptogenesis after the onset of neurogenesis, it is also capable of pushing neural stem cells to exit the cell cycle and become neuronal progenitors. Similar cell- and developmental stage-specific roles of miRNAs have been described before for other brain-enriched miRNAs such as in the case of miR-134.[62]

Among the novel validated miR-34a targets that we elucidated here, ANK3 is localized at the axon initial segment,[63,64] and recent findings have reported that it selectively decreased in the cerebellum of BD patients,[45] the same brain region we observed to show elevated miR-34a levels in the present study. In addition, CACNB3 is involved in the regulation of surface expression and gating of the α-subunit (CACNA1C),[65] which has also been recently reported to be downregulated in the cerebellum of BD patients,[44] (SJH, manuscript in preparation), and shown here to be indirectly affected by miR-34a overexpression as part of the NanoString profiling. Finally, in the brain, DDN is a postsynaptic component of cytoskeletal modifications at the synapse that interacts with α-actinin and whose mRNA is localized to the synapse through a specific 3′UTR.[66] Therefore, the newly validated targets of miR-34a uncovered in our study are strongly linked to neuronal structure and function. Not surprisingly, when we analyzed miR-34a-predicted targets for gene ontology parameters, we found that molecular networks related to neuronal development, differentiation and synaptic plasticity were among the top significant results (Supplementary Tables S3–S6). In addition, the same *in silico* analysis revealed autism together with schizophrenia and depressive disorder among the top five diseases enriched in miR-34a-predicted targets (Supplementary Table S7). The validation of miR-34a targets through luciferase assays was supported by correlation data between miR-34a and its mRNA targets *ANK3* and *CACNB3*. Despite these negative correlations, it is very likely that additional miRNAs or additional factors could be responsible for the changes in the levels of the targets during development.[67] It also has to be taken into account, though, that miRNAs and their targets are often in complex regulatory loops, and the impact of miRNA-mediated inhibition can vary coherent and incoherent interactions,[3,68,69] so that anti-correlated expression is not a prerequisite for miRNA targeting.

Chronic treatment with either lithium or valproic acid, which are the most effective mood stabilizers, reduces miR-34a expression *in vivo* and in neuronal cultures.[25] On a similar note, chronic lithium and valproic acid co-treatment has been reported to downregulate miR-34a levels in rodent cerebellar granule cell cultures.[24] On the other hand, lithium treatment appears to have opposite effects in miR-34a expression in human peripheral blood-

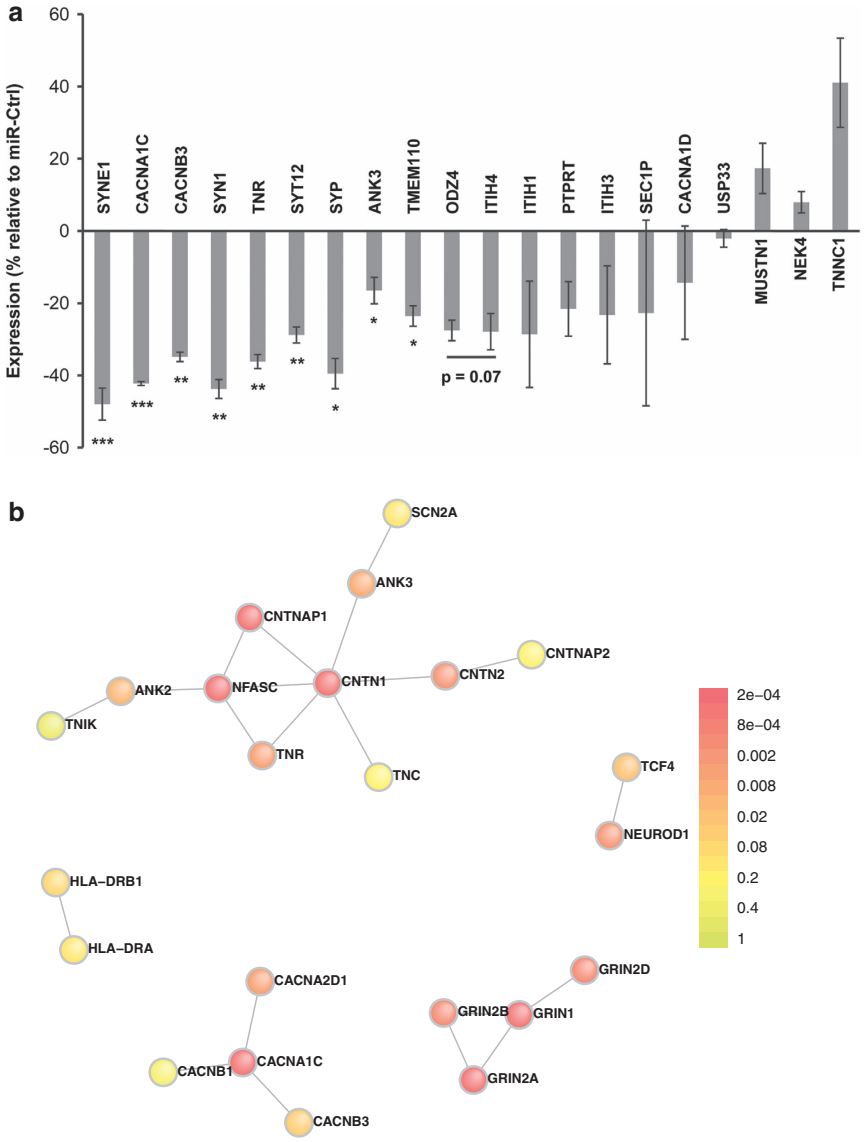

Figure 4. miR-34a overexpression affects BD-risk genes that are highly connected through a protein interaction network. (**a**) Data show the expression of 18 BD-risk genes (*SYNE1*, *CACNA1C*, *CACNB3*, *TNR*, *SYT12*, *ANK3*, *TMEM110*, *ODZ4*, *ITIH4*, *ITIH1*, *PTPRT*, *ITIH3*, *SEC1P*, *CACNA1D*, *USP33*, *MUSTN1*, *NEK4* and *TNCC1*) and two validated miR-34a targets (*SYN1* and *SYT*) measured in 6-week differentiated neurons overexpressing either miR-Ctrl or miR-34a. Data are expressed in percentage relative to miR-Ctrl overexpressing neurons with $n = 3$ replicates. $^{*}P < 0.05$, $^{**}P < 0.01$, $^{***}P < 0.001$ compared with miR-Ctrl treatment based on a two-tailed, one-sample *t*-test. (**b**) Direct protein–protein interactions among genes differentially affected by miR-34a overexpression over a neurodevelopmental time course ($t = 0$, 2, 4 and 8 weeks in duplicate; $t = 6$ weeks in triplicate) in human induced pluripotent stem cell-derived neuronal progenitor cells visualized using DAPPLE v2.0. Color coding corresponds to *P*-value from 5000 within-degree, node-label permutations. See Supplementary Text for additional details.

derived, lymphoblastoid cell lines.[55] More importantly, miR-34a has been shown in non-neuronal cells to be a strong inhibitor of WNT signaling and β-catenin-mediated transcription in response to p53 activation in non-neuronal cells.[70,71] Recent findings have demonstrated that ANK3 regulates both cadherin and WNT signaling pathways by altering the availability of β-catenin with ANK3 loss-of-function impacting neurogenesis,[72] supporting the importance of WNT signaling in the etiology of neurodevelopmental disorders. Given the effects of lithium on WNT signaling, it is therefore intriguing to speculate that high miR-34a expression could be important for the pathophysiology of BD through this pathway and that the delayed therapeutic effects of mood stabilizers could be partly attributed to their capacity to reduce miR-34a levels following chronic treatment.

We find our observation of selective dysregulation of miR-34a in the cerebellum consistent, with growing evidence from the work of others and us demonstrating the selective dysregulation of genes implicated in BD etiology specifically in the cerebellum, namely ANK3 and CACNA1C, that have recently been reported[44,45] (SJH, manuscript in preparation). Although the PFC remains a brain region commonly implicated in BD pathophysiology, the potential importance of the cerebellum in BD and other affective disorders is increasingly apparent, with recent neuroimaging studies having revealed complex connectivity with the cerebral cortex.[46,47,52,53,73] Given the well-known topographical organization of the cerebellum into specialized regions, including those critical to affective processing,[73] future work in cerebellar subregions could help determine whether miR-34a expression is

dysregulated in areas implicated in control of emotional and affective behavior and whether these expression differences correlate with the selective dysregulated expression of *ANK3* and *CACNA1C* that has also been observed in the postmortem cerebellum samples.[44,45]

Though we did not see any differences in miR-34a expression in PFC nor anterior cingulate cortex of BD patients compared with control individuals, we note that a recent study on the PFC from 15 BD patient samples and 15 non-psychiatric controls reported a modest 0.84-fold downregulation of miR-34a in PFC of BD patients relative to controls,[74] and another study reported no difference.[75] Such discrepancies in gene expression between postmortem brain cohorts may be due to disease heterogeneity and possible methodological reasons. Future studies with additional cohorts are needed to replicate our findings and to determine whether miR-34a alterations in BD are widespread in the brain or limited to specific brain regions as we observed. Addressing these questions will benefit from access to high-quality postmortem brain tissue collections of sizes commensurate with the known phenotypic genetic heterogeneity of the disorder, along with sub-regional and ideally cell subtype specific. Being able to generate defined neuronal subtypes (for example, cerebellar neurons) with authentic patterning of the human brain will allow explicit test of the correlation between *in vitro* cellular models and postmortem observations, the absence of which is a limitation of our current study.

Although our studies employed a total of eight (five BD cases, three controls) iNs and two (familial control and BD son) iPSCs, future studies with additional cohorts of well phenotyped BD patient and control fibroblasts reprogrammed into iNs and iPSCs are needed to determine whether miR-34a alterations in BD are common among all BD patients. These studies are likely to benefit from incorporation of a wider spectrum of neuropsychiatric disorder patients to understand how commonly variation in miR-34a is observed among patients with major depression, schizophrenia and other disorders.

In summary, our study has implicated miR-34a as a small non-coding RNA dysregulated in BD that regulates multiple known BD-linked genes and can affect the *in vitro* differentiation of human neurons. Further studies examining the regional expression and regulation of miR-34a-sensitive networks will provide critically needed insight into the pathogenesis of BD and may help elucidate new pathways for targeted therapeutic development.

ACKNOWLEDGMENTS

We thank the Stanley Medical Research Institute (Dr Maree Webster) for providing RNA and tissue samples from their postmortem human brain collection, the Crabtree laboratory, especially Dr Alfred Sun, for contributing plasmids and help with the iN protocol and Dr Colm O'Dushlaine for his help with miR-34a target prediction. This work was supported through funding from the Swiss National Science Foundation, the Stanley Medical Research Institute and the National Institute of Mental Health (R21MH093958, R33MH087896, R01MH091115, R01MH095088).

REFERENCES

1 Ketter TA. Diagnostic features, prevalence, and impact of bipolar disorder. *J Clin Psychiatry* 2010; **71**: e14.
2 Craddock N, Sklar P. Genetics of bipolar disorder. *Lancet* 2013; **381**: 1654–1662.
3 Bartel DP. MicroRNAs: target recognition and regulatory functions. *Cell* 2009; **136**: 215–233.
4 Krichevsky AM, King KS, Donahue CP, Khrapko K, Kosik KS. A microRNA array reveals extensive regulation of microRNAs during brain development. *RNA* 2003; **9**: 1274–1281.
5 Krol J, Loedige I, Filipowicz W. The widespread regulation of microRNA biogenesis, function and decay. *Nat Rev Genetics* 2010; **11**: 597–610.
6 Mellios N, Sur M. The emerging role of microRNAs in schizophrenia and autism spectrum disorders. *Front Psychiatry* 2012; **3**: 39.
7 Schratt G. microRNAs at the synapse. *Nat Rev Neurosci* 2009; **10**: 842–849.
8 Green MJ, Cairns MJ, Wu J, Dragovic M, Jablensky A, Tooney PA *et al.* Genome-wide supported variant MIR137 and severe negative symptoms predict membership of an impaired cognitive subtype of schizophrenia. *Mol Psychiatry* 2013; **18**: 774–780.
9 Miller BH, Wahlestedt C. MicroRNA dysregulation in psychiatric disease. *Brain Res* 2010; **1338**: 89–99.
10 O'Connor RM, Dinan TG, Cryan JF. Little things on which happiness depends: microRNAs as novel therapeutic targets for the treatment of anxiety and depression. *Mol Psychiatry* 2012; **17**: 359–376.
11 Xu B, Karayiorgou M, Gogos JA. MicroRNAs in psychiatric and neurodevelopmental disorders. *Brain Res* 2010; **1338**: 78–88.
12 Fenelon K, Mukai J, Xu B, Hsu PK, Drew LJ, Karayiorgou M *et al.* Deficiency of Dgcr8, a gene disrupted by the 22q11.2 microdeletion, results in altered short-term plasticity in the prefrontal cortex. *Proc Natl Acad Sci USA* 2011; **108**: 4447–4452.
13 Fenelon K, Xu B, Lai CS, Mukai J, Markx S, Stark KL *et al.* The pattern of cortical dysfunction in a mouse model of a schizophrenia-related microdeletion. *J Neurosci* 2013; **33**: 14825–14839.
14 Stark KL, Xu B, Bagchi A, Lai WS, Liu H, Hsu R *et al.* Altered brain microRNA biogenesis contributes to phenotypic deficits in a 22q11-deletion mouse model. *Nat Genetics* 2008; **40**: 751–760.
15 Xu B, Hsu PK, Stark KL, Karayiorgou M, Gogos JA. Derepression of a neuronal inhibitor due to miRNA dysregulation in a schizophrenia-related microdeletion. *Cell* 2013; **152**: 262–275.
16 Psychiatric GWAS Consortium Bipolar Disorder Working Group: Sklar P, Ripke S, Scott LJ, Andreassen OA, Cichon S, Craddock N *et al.* Large-scale genome-wide association analysis of bipolar disorder identifies a new susceptibility locus near ODZ4. *Nat Genetics* 2011; **43**: 977–983.
17 Muinos-Gimeno M, Espinosa-Parrilla Y, Guidi M, Kagerbauer B, Sipila T, Maron E *et al.* Human microRNAs miR-22, miR-138-2, miR-148a, and miR-488 are associated with panic disorder and regulate several anxiety candidate genes and related pathways. *Biol Psychiatry* 2011; **69**: 526–533.
18 Saba R, Schratt GM. MicroRNAs in neuronal development, function and dysfunction. *Brain Res* 2010; **1338**: 3–13.
19 Schizophrenia Psychiatric Genome-Wide Association Study (GWAS) Consortium: Ripke S, Sanders AR, Kendler KS, Levinson DF, Sklar P, Holmans PA *et al.* Genome-wide association study identifies five new schizophrenia loci. *Nat Genetics* 2011; **43**: 969–976.
20 Kwon E, Wang W, Tsai LH. Validation of schizophrenia-associated genes CSMD1, C10orf26, CACNA1C and TCF4 as miR-137 targets. *Mol Psychiatry* 2013; **18**: 11–12.
21 Cummings E, Donohoe G, Hargreaves A, Moore S, Fahey C, Dinan TG *et al.* Mood congruent psychotic symptoms and specific cognitive deficits in carriers of the novel schizophrenia risk variant at MIR-137. *Neurosci Lett* 2013; **532**: 33–38.
22 Lett TA, Chakavarty MM, Felsky D, Brandl EJ, Tiwari AK, Goncalves VF *et al.* The genome-wide supported microRNA-137 variant predicts phenotypic heterogeneity within schizophrenia. *Mol Psychiatry* 2013; **18**: 443–450.
23 Ripke S, O'Dushlaine C, Chambert K, Moran JL, Kahler AK, Akterin S *et al.* Genome-wide association analysis identifies 13 new risk loci for schizophrenia. *Nat Genetics* 2013; **45**: 1150–1159.
24 Hunsberger JG, Fessler EB, Chibane FL, Leng Y, Maric D, Elkahloun AG *et al.* Mood stabilizer-regulated miRNAs in neuropsychiatric and neurodegenerative diseases: identifying associations and functions. *Am J Transl Res* 2013; **5**: 450–464.
25 Zhou R, Yuan P, Wang Y, Hunsberger JG, Elkahloun A, Wei Y *et al.* Evidence for selective microRNAs and their effectors as common long-term targets for the actions of mood stabilizers. *Neuropsychopharmacology* 2009; **34**: 1395–1405.
26 Agostini M, Tucci P, Steinert JR, Shalom-Feuerstein R, Rouleau M, Aberdam D *et al.* microRNA-34a regulates neurite outgrowth, spinal morphology, and function. *Proc Natl Acad Sci USA* 2011; **108**: 21099–21104.
27 Agostini M, Tucci P, Killick R, Candi E, Sayan BS, Rivetti di Val Cervo P *et al.* Neuronal differentiation by TAp73 is mediated by microRNA-34a regulation of synaptic protein targets. *Proc Natl Acad Sci USA* 2011; **108**: 21093–21098.
28 Chi SW, Zang JB, Mele A, Darnell RB. Argonaute HITS-CLIP decodes microRNA-mRNA interaction maps. *Nature* 2009; **460**: 479–486.
29 Wibrand K, Pai B, Siripornmongcolchai T, Bittins M, Berentsen B, Ofte ML *et al.* MicroRNA regulation of the synaptic plasticity-related gene Arc. *PLoS One* 2012; **7**: e41688.
30 Muhleisen TW, Leber M, Schulze TG, Strohmaier J, Degenhardt F, Treutlein J *et al.* Genome-wide association study reveals two new risk loci for bipolar disorder. *Nat Commun* 2014; **5**: 3339.
31 Sheridan SD, Theriault KM, Reis SA, Zhou F, Madison JM, Daheron L *et al.* Epigenetic characterization of the FMR1 gene and aberrant neurodevelopment in human induced pluripotent stem cell models of fragile X syndrome. *PLoS One* 2011; **6**: e26203.

32 Madison JM, Zhou F, Nigam A, Hussain A, Barker DD, Nehme R *et al.* Characterization of bipolar disorder patient-specific induced pluripotent stem cells from a family reveals neurodevelopmental and mRNA expression abnormalities. *Molecular Psychiatry*, 2015 (in press).
33 Spitzer RL, Williams JB, Gibbon M, First MB. The structured clinical interview for DSM-III-R (SCID). I: History, rationale, and description. *Arch Gen Psychiatry* 1992; **49**: 624–629.
34 Yoo AS, Sun AX, Li L, Shcheglovitov A, Portmann T, Li Y *et al.* MicroRNA-mediated conversion of human fibroblasts to neurons. *Nature* 2011; **476**: 228–231.
35 Dweep H, Sticht C, Pandey P, Gretz N. miRWalk--database: prediction of possible miRNA binding sites by "walking" the genes of three genomes. *J Biomed Informatics* 2011; **44**: 839–847.
36 Griffiths-Jones S, Grocock RJ, van Dongen S, Bateman A, Enright AJ. miRBase: microRNA sequences, targets and gene nomenclature. *Nucleic Acids Res* 2006; **34**: D140–D144.
37 Krek A, Grun D, Poy MN, Wolf R, Rosenberg L, Epstein EJ *et al.* Combinatorial microRNA target predictions. *Nat Genetics* 2005; **37**: 495–500.
38 Lewis BP, Burge CB, Bartel DP. Conserved seed pairing, often flanked by adenosines, indicates that thousands of human genes are microRNA targets. *Cell* 2005; **120**: 15–20.
39 Maragkakis M, Reczko M, Simossis VA, Alexiou P, Papadopoulos GL, Dalamagas T *et al.* DIANA-microT web server: elucidating microRNA functions through target prediction. *Nucleic Acids Res* 2009; **37**: W273–W276.
40 Miranda KC, Huynh T, Tay Y, Ang YS, Tam WL, Thomson AM *et al.* A pattern-based method for the identification of MicroRNA binding sites and their corresponding heteroduplexes. *Cell* 2006; **126**: 1203–1217.
41 Rehmsmeier M, Steffen P, Hochsmann M, Giegerich R. Fast and effective prediction of microRNA/target duplexes. *RNA* 2004; **10**: 1507–1517.
42 Wang X. miRDB: a microRNA target prediction and functional annotation database with a wiki interface. *RNA* 2008; **14**: 1012–1017.
43 Huang da W, Sherman BT, Tan Q, Kir J, Liu D, Bryant D *et al.* DAVID bioinformatics resources: expanded annotation database and novel algorithms to better extract biology from large gene lists. *Nucleic Acids Res* 2007; **35**: W169–W175.
44 Gershon ES, Grennan K, Busnello J, Badner JA, Ovsiew F, Memon S *et al.* A rare mutation of CACNA1C in a patient with bipolar disorder, and decreased gene expression associated with a bipolar-associated common SNP of CACNA1C in brain. *Mol Psychiatry* 2013; **19**: 890–894.
45 Rueckert EH, Barker D, Ruderfer D, Bergen SE, O'Dushlaine C, Luce CJ *et al.* Cis-acting regulation of brain-specific ANK3 gene expression by a genetic variant associated with bipolar disorder. *Mol Psychiatry* 2013; **18**: 922–929.
46 Baldacara L, Nery-Fernandes F, Rocha M, Quarantini LC, Rocha GG, Guimaraes JL *et al.* Is cerebellar volume related to bipolar disorder? *J Affect Disord* 2011; **135**: 305–309.
47 Buckner RL. The cerebellum and cognitive function: 25 years of insight from anatomy and neuroimaging. *Neuron* 2013; **80**: 807–815.
48 Eker C, Simsek F, Yilmazer EE, Kitis O, Cinar C, Eker OD *et al.* Brain regions associated with risk and resistance for bipolar I disorder: a voxel-based MRI study of patients with bipolar disorder and their healthy siblings. *Bipolar Disord* 2014; **16**: 249–261.
49 Kim D, Byul Cho H, Dager SR, Yurgelun-Todd DA, Yoon S, Lee JH *et al.* Posterior cerebellar vermal deficits in bipolar disorder. *J Affect Disord* 2013; **150**: 499–506.
50 Liang MJ, Zhou Q, Yang KR, Yang XL, Fang J, Chen WL *et al.* Identify changes of brain regional homogeneity in bipolar disorder and unipolar depression using resting-state FMRI. *PLoS One* 2013; **8**: e79999.
51 Smolin B, Karry R, Gal-Ben-Ari S, Ben-Shachar D. Differential expression of genes encoding neuronal ion-channel subunits in major depression, bipolar disorder and schizophrenia: implications for pathophysiology. *Int J Neuropsychopharmacol* 2012; **15**: 869–882.
52 Soontornniyomkij B, Everall IP, Chana G, Tsuang MT, Achim CL, Soontornniyomkij V. Tyrosine kinase B protein expression is reduced in the cerebellum of patients with bipolar disorder. *J Affect Disord* 2011; **133**: 646–654.
53 Cross-Disorder Group of the Psychiatric Genomics Consortium: Smoller JW, Ripke S, Lee PH, Neale B, Nurnberger JI, Santangelo S *et al.* The cerebellum and neuropsychiatric disorders. *Psychiatry Res* 2012; **198**: 527–532.
54 Identification of risk loci with shared effects on five major psychiatric disorders: a genome-wide analysis. *Lancet* 2013; **381**: 1371–1379.
55 Chen H, Wang N, Burmeister M, McInnis MG. MicroRNA expression changes in lymphoblastoid cell lines in response to lithium treatment. *Int J Neuropsychopharmacol* 2009; **12**: 975–981.
56 Du J, Wei Y, Liu L, Wang Y, Khairova R, Blumenthal R *et al.* A kinesin signaling complex mediates the ability of GSK-3beta to affect mood-associated behaviors. *Proc Natl Acad Sci USA* 2010; **107**: 11573–11578.
57 Ferrandiz-Huertas C, Gil-Minguez M, Lujan R. Regional expression and subcellular localization of the voltage-gated calcium channel beta subunits in the developing mouse brain. *J Neurochem* 2012; **122**: 1095–1107.
58 Huang Y, Zou Q, Song H, Song F, Wang L, Zhang G *et al.* A study of miRNAs targets prediction and experimental validation. *Protein Cell* 2010; **1**: 979–986.
59 Kuhn DE, Martin MM, Feldman DS, Terry AV Jr., Nuovo GJ, Elton TS. Experimental validation of miRNA targets. *Methods* 2008; **44**: 47–54.
60 Aranha MM, Santos DM, Sola S, Steer CJ, Rodrigues CM. miR-34a regulates mouse neural stem cell differentiation. *PLoS One* 2011; **6**: e21396.
61 Fineberg SK, Datta P, Stein CS, Davidson BL. MiR-34a represses Numbl in murine neural progenitor cells and antagonizes neuronal differentiation. *PLoS One* 2012; **7**: e38562.
62 Gaughwin P, Ciesla M, Yang H, Lim B, Brundin P. Stage-specific modulation of cortical neuronal development by Mmu-miR-134. *Cereb Cortex* 2011; **21**: 1857–1869.
63 Clark BA, Monsivais P, Branco T, London M, Hausser M. The site of action potential initiation in cerebellar Purkinje neurons. *Nat Neurosci* 2005; **8**: 137–139.
64 Komada M, Soriano P. [Beta]IV-spectrin regulates sodium channel clustering through ankyrin-G at axon initial segments and nodes of Ranvier. *J Cell Biol* 2002; **156**: 337–348.
65 Yamaguchi H, Hara M, Strobeck M, Fukasawa K, Schwartz A, Varadi G. Multiple modulation pathways of calcium channel activity by a beta subunit. Direct evidence of beta subunit participation in membrane trafficking of the alpha1C subunit. *J Biol Chem* 1998; **273**: 19348–19356.
66 Kremerskothen J, Kindler S, Finger I, Veltel S, Barnekow A. Postsynaptic recruitment of Dendrin depends on both dendritic mRNA transport and synaptic anchoring. *J Neurochem* 2006; **96**: 1659–1666.
67 Mellios N, Huang HS, Grigorenko A, Rogaev E, Akbarian S. A set of differentially expressed miRNAs, including miR-30a-5p, act as post-transcriptional inhibitors of BDNF in prefrontal cortex. *Hum Mol Genetics* 2008; **17**: 3030–3042.
68 Liu H, Kohane IS. Tissue and process specific microRNA-mRNA co-expression in mammalian development and malignancy. *PLoS One* 2009; **4**: e5436.
69 Osella M, Bosia C, Cora D, Caselle M. The role of incoherent microRNA-mediated feedforward loops in noise buffering. *PLoS Comput Biol* 2011; **7**: e1001101.
70 Hashimi ST, Fulcher JA, Chang MH, Gov L, Wang S, Lee B. MicroRNA profiling identifies miR-34a and miR-21 and their target genes JAG1 and WNT1 in the coordinate regulation of dendritic cell differentiation. *Blood* 2009; **114**: 404–414.
71 Kim NH, Kim HS, Kim NG, Lee I, Choi HS, Li XY *et al.* p53 and microRNA-34 are suppressors of canonical Wnt signaling. *Sci Signal* 2011; **4**: ra71.
72 Durak O, de Anda FC, Singh KK, Leussis MP, Petryshen TL, Sklar P *et al.* Ankyrin-G regulates neurogenesis and Wnt signaling by altering the subcellular localization of beta-catenin. *Mol Psychiatry* 2014; advance online publication, 13 May 2014; doi:10.1038/mp.2014.42.
73 Stoodley CJ, Schmahmann JD. Evidence for topographic organization in the cerebellum of motor control versus cognitive and affective processing. *Cortex* 2010; **46**: 831–844.
74 Smalheiser NR, Lugli G, Zhang H, Rizavi H, Cook EH, Dwivedi Y. Expression of microRNAs and other small RNAs in prefrontal cortex in schizophrenia, bipolar disorder and depressed subjects. *PLoS One* 2014; **9**: e86469.
75 Kim AH, Reimers M, Maher B, Williamson V, McMichael O, McClay JL *et al.* MicroRNA expression profiling in the prefrontal cortex of individuals affected with schizophrenia and bipolar disorders. *Schizophr Res* 2010; **124**: 183–191.

Supplementary Information accompanies the paper on the Molecular Psychiatry website (http://www.nature.com/mp)